

DreamLite : A Lightweight On-Device Unified Model for Image Generation and Editing

Kailai Feng, Yuxiang Wei[†], Bo Chen, Yang Pan, Hu Ye, Songwei Liu,
Chenqian Yan, Yuan Gao[†]

Intelligent Creation Lab, ByteDance

[†]Corresponding Author

Abstract

Diffusion models have made significant progress in both text-to-image (T2I) generation and text-guided image editing. However, these models are typically built with billions of parameters, leading to high latency and increased deployment challenges. While on-device diffusion models improve efficiency, they largely focus on T2I generation and lack support for image editing. In this paper, we propose DreamLite, a **compact unified on-device diffusion model (0.39B)** that supports both T2I generation and text-guided image editing within a single network. DreamLite is built on a pruned mobile U-Net backbone and unifies conditioning through in-context spatial concatenation in the latent space. It concatenates images horizontally as input, using a (target | blank) configuration for generation tasks and (target | source) for editing tasks. To stabilize the training of this compact model, we introduce a task-progressive joint pretraining strategy that sequentially targets T2I, editing, and joint tasks. After high-quality SFT and reinforcement learning, DreamLite achieves GenEval (0.72) for image generation and ImgEdit (4.11) for image editing, outperforming existing on-device models and remaining competitive with several server-side models. By employing step distillation, we further reduce denoising processing to just 4 steps, enabling our DreamLite could generate or edit a 1024×1024 image in less than 1s on a Xiaomi 14 smartphone. To the best of our knowledge, DreamLite is the first unified on-device diffusion model that supports both image generation and image editing.

Date: March 30, 2026

Project Page: <https://carlofkl.github.io/dreamlite/>

1 Introduction

Recent advancements in large-scale diffusion models, such as FLUX series [23, 25], HunyuanImage 3.0 [7], Qwen Image [51] and Seedream series [12, 15, 44] have achieved remarkable progress in both text-to-image (T2I) generation and text-guided editing (I2I). Despite their superior semantic alignment and visual fidelity, these models typically rely on massive backbones with billions of parameters and iterative denoising processes. For instance, FLUX [25] scales its DiT backbone to 12B parameters, imposing prohibitive memory requirements and high inference latency that preclude efficient deployment on consumer-grade devices. To enhance efficiency, recent research has explored lightweight architectures such as SANA [55], DeepGen1.0 [50] and VIBE [1], which typically utilize backbones on the order of ~ 2 B parameters. However, achieving stable, real-time performance with these models on mobile hardware remains a significant challenge.

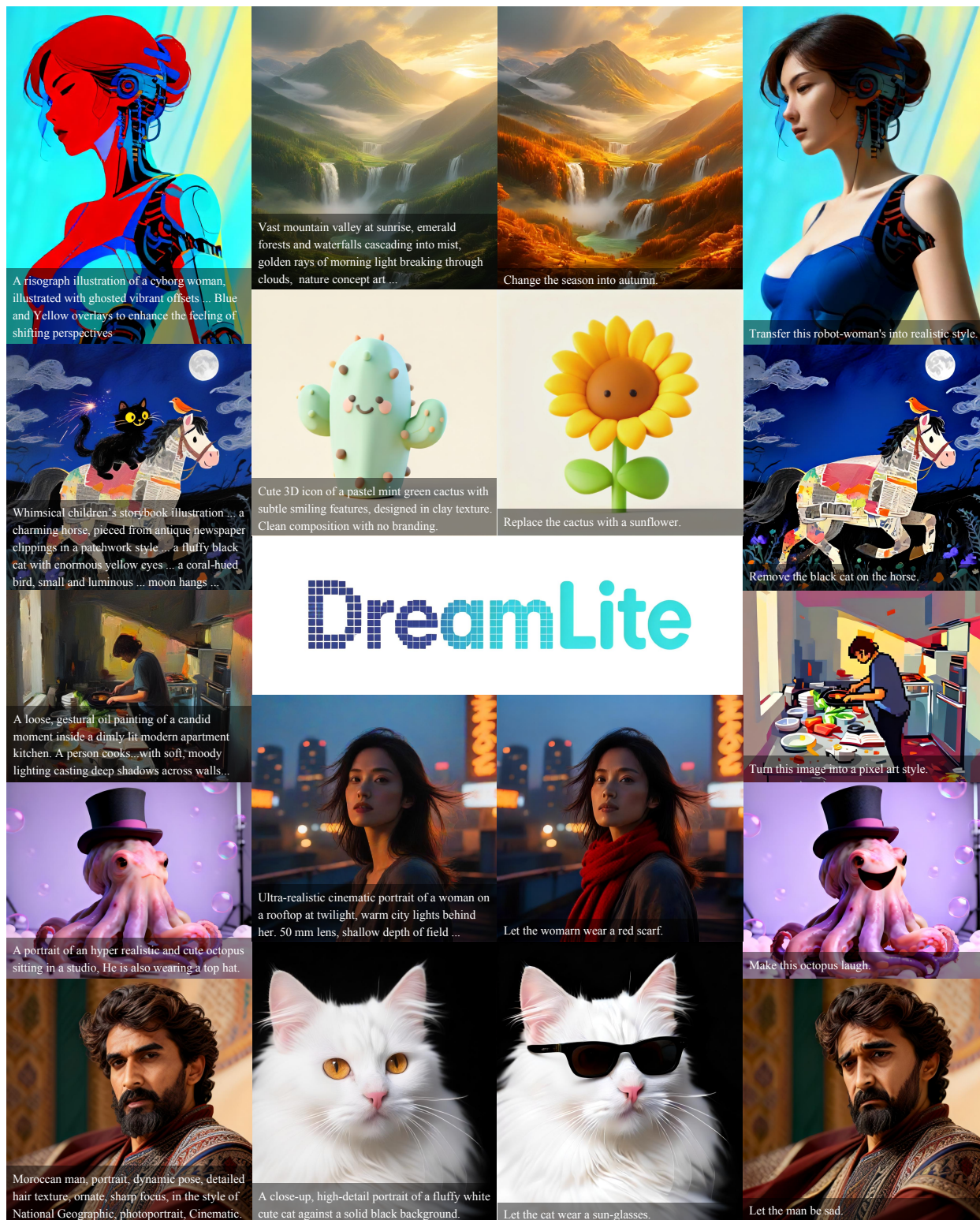


Figure 1 Generation (left) and Editing (right) examples of DreamLite.

To improve accessibility, several works [17, 18, 27, 62] focus on deploying compact diffusion models directly on mobile devices. For example, SnapFusion [27], Mobile Diffusion [62] and SnapGen [17] leverage lightweight U-Net backbones to achieve quality–efficiency trade-offs for on-device T2I generation. More recently, SnapGen++ [18] has explored the potential of Diffusion Transformer for efficient mobile generation. However, these approaches predominantly focus on T2I generation and lack support for image editing. In practice, creators demand a unified experience that seamlessly integrates “generate” and “edit” functionalities within a single application. Furthermore, deploying two separate models significantly increases system complexity and resource consumption, particularly in memory-constrained devices.

In this paper, we introduce DreamLite, a unified and compact diffusion model capable of performing both image generation and editing within a single network. Following SnapGen [17], we adopt a pruned UNet backbone and extend it for multi-task learning via an in-context conditioning mechanism. Specifically, we spatially concatenate the target and condition images (left-right) at the input level. For generation, the target is paired with a blank image; for editing, it is paired with the source image. To resolve task ambiguity, we prepend explicit task tokens (*i.e.*, [Generate] or [Edit]) to the text prompts. This design enable effective task routing within a shared parameter space without introducing additional parameters or specialized branches.

Training the compact model with a unified scheme is challenging due to its limited capacity and the divergent optimization objectives of generation and editing tasks. To ensure stability, we propose a task-progressive joint pretraining scheme. Specifically, we introduce an intermediate editing pretraining stage between text-to-image pretraining and joint training. This stage aligns visual condition with the generative latent space prior to complex unified joint optimization, thereby facilitating stable training. Consequently, the pretraining of DreamLite is divided into three progressive stages: *i.e.*, T2I Pretraining → Editing Training → Unified Joint Training. Following this, we further adopt a two-stage post-training strategy: supervised fine-tuning (SFT) on a curated high-quality dataset, followed by reinforcement learning (RL) for preference alignment. During RL training, we employ HPSv3 [36] as the reward model for generation and EditReward [53] for editing, optimizing the diffusion model via ReFL [56]. This post-training phase consistently enhances both perceptual quality and instruction following, enabling our compact model to outperform prior on-device diffusion baselines.

Overall, DreamLite achieves GenEval (0.72) and DPG (85.8) for text-to-image generation, along with ImgEdit (4.11) and GEdit (6.88) for text-guided image editing. It outperforms specialized lightweight baselines such as SnapGen, SANA-0.6B and VIBE while remaining competitive with larger unified models such as OmniGen2 and Bagel. These results validate the efficacy of our unified architecture. To minimize deployment overhead, we apply DMD2 [59] to compress the sampling process into 4 denoising steps. On a representative smartphone (*i.e.*, Xiaomi 14), DreamLite completes a 1024×1024 generation or editing task in less than 1 second. To the best of our knowledge, DreamLite is the first unified on-device diffusion model to support both generation and editing within a single network for mobile deployment.

Our contributions are summarized as follows:

- We propose, to the best of our knowledge, the first unified on-device model that supports both text-to-image generation and text-based image editing, eliminating the need to deploy two separate models.
- We introduce an in-context conditioning mechanism for UNet to unify generation and editing, and propose a task-progressive joint pretraining scheme (*i.e.*, T2I → Edit → Unified Joint Training) to stably train the model.
- DreamLite achieves competitive performance on standard benchmarks and consistently outperforms prior mobile models. After deployment on Xiaomi 14, DreamLite could generate or edit a 1024×1024 image in less than 1s.

2 Related Work

2.1 Unified Generative Models

Large-scale image models are increasingly built as unified generative systems that support both text-to-image generation and instruction-based editing through a single model. Recent model families such as FLUX 2 [24], HunyuanImage [7], Seedream 4.0 [44], Qwen-Image-2 [51], as well as commercial systems like Gemini-Image [38], GPT-Image [16], LongCat-Image [48] and DeepGen [50], all move toward “generate + edit” as first-class capabilities, typically by strengthening text-image alignment and instruction following with large backbones and curated post-training. A representative line is FLUX.2, which frames unified generation and editing via an in-context formulation. Compared to these large or cloud-oriented unified systems, our work targets a *single compact* diffusion model that supports both generation and instruction-based editing for *on-device* deployment under strict memory/latency constraints.

2.2 Efficient Diffusion Models

A growing body of work improves diffusion efficiency by optimizing architectures, attention mechanisms, and training/inference recipes. PixArt- Σ [8] explores transformer efficiency for high-resolution generation with key-value compression to alleviate attention cost at large token counts. And SANA [55] proposes linear-attention diffusion transformers to reduce the quadratic complexity of self-attention at high resolutions while maintaining competitive generation performance. Beyond pure generation, EditMGT [9] and VIBE [1] presents a compact instruction-based editing pipeline that combines a lightweight vision-language model with an efficient diffusion backbone, demonstrating that strong editing can be achieved without relying on extremely large diffusion models. Our method is complementary to these efforts: rather than only accelerating T2I or only optimizing editing, we focus on an efficient *unified* interface that consolidates T2I and editing into a single compact model.

2.3 On-Device Generative Models

To enable on-device deployment, prior works have explored quantization, pruning, and knowledge distillation to reduce model size and latency. Early on-device systems [27, 62] pruned and distilled U-Net architectures to generate 512-pixel images within seconds. SnapGen [17] demonstrated that a compact U-Net derived from SDXL can generate 1024×1024 images on mobile devices with a carefully engineered architecture and training recipe. More recently, SnapGen++ [18] explores efficient diffusion transformers tailored for mobile and edge deployment. Concurrent to our work, Mobile-O [45] attempts to unify both visual generation and understanding within a single compact framework. However, since Mobile-O relies on an understanding-centric paradigm to execute generation tasks, it struggles with fine-grained visual control and spatial consistency at in editing tasks. Consequently, its performance in complex image editing scenarios remains somewhat suboptimal. Despite this progress, most on-device works primarily emphasize T2I generation, while instruction-based editing often requires either separate models or additional editing-specific components. Our work targets this gap by providing a unified interface and training strategy so that a single compact model supports both “generate an image” and “edit my photo,” reducing deployment complexity and resource consumption on mobile devices.

2.4 RLHF

Post-training alignment has emerged as a crucial stage for enhancing perceptual quality and instruction compliance, surpassing the limitations of noisy web-scale pre-training. A common practice involves utilizing learned reward models (*e.g.*, ImageReward [56], HPSv2/v3 [36, 54], PickScore [22], and the editing-specific EditReward [53]) as optimization targets to improve aesthetics and prompt faithfulness while mitigating visual artifacts. On the optimization front, various methods adapt reinforcement learning (RL) to generative models. For instance, ReFL [56] performs reward-guided fine-tuning for diffusion models under constrained backprop settings to reduce training cost, and has inspired follow-up explorations of more efficient preference optimization. Parallel to RL-based approaches, DPO-like objectives (*e.g.*, Diffusion-DPO [49], AlignProp [40]) have been developed to leverage pairwise preferences without explicit reward modeling. Recent flow-model

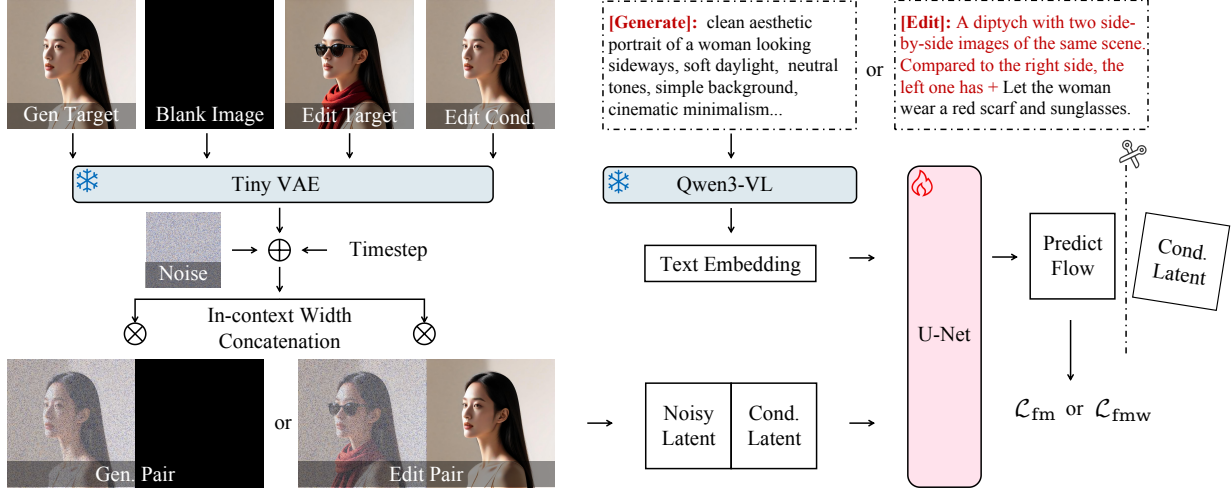


Figure 2 Overview of DreamLite architecture. It consists of three primary modules: a UNet backbone, a Variational Autoencoder (VAE), and a text encoder. To support unified generation and editing, an in-context conditioning framework is adopted that unifies both tasks at the input level.

works also explore GRPO variants (*e.g.*, Flow-GRPO [30], DanceGRPO [57]) for better stability and instruction following under preference feedback.

2.5 Step Distillation

Few-step sampling is essential for interactive and on-device applications. A representative line is consistency-based distillation, including Latent Consistency Models (LCM) [33], which distill time-consistent behavior to enable generation in a small number of steps. Another influential family is distribution matching distillation. DMD [60] distills a multi-step teacher into a few-step student via distribution matching objectives, and DMD2 [59] further improves stability and sample quality under aggressive step reduction. In practice, these methods are often used to compress sampling to $\leq 4-8$ steps with acceptable quality, and have been integrated into various backbones (including SD, SDXL and QwenImage, *etc.*). Adversarial-based distillation is also a prominent approach; for instance, SDXL-Turbo and SD-Turbo [42] utilize Adversarial Diffusion Distillation (ADD) to achieve high-fidelity, real-time synthesis in a single step. Recent efforts such as RG-LCD [26] and DI++ [34] incorporate reward model into the distillation process with an additional score model to maintain proximity to the original generator. To address this, LaSRO [21] optimizes arbitrary rewards via latent space exploration. Reward-Instruct [35] aligns generators with rewards without requiring training images. TAFS-GRPO [61] eliminates the need for differentiable reward functions by leveraging a policy gradient algorithm. In this work, we employ the DMD2 to compress our sampling process to 4 steps.

3 Method

This section presents the training pipeline and details of our DreamLite. We first describe the model architecture (Section 3.1), and then detail our training procedure, including task-progressive joint pretraining (Section 3.2), post training (Section 3.3), and few-step distillation (Section 3.4).

3.1 Model Architecture

As illustrated in Fig. 2, the architecture of DreamLite consists of three primary modules: a UNet backbone, a Variational Autoencoder (VAE), and a text encoder. To support unified image generation and editing, we further introduce the in-context conditioning mechanism.

Variational Autoencoder. Following [23, 41], we adopt a latent diffusion framework. To enable efficient on-device deployment, we employ an extremely lightweight VAE (*i.e.*, TinyVAE [37]), which contains only

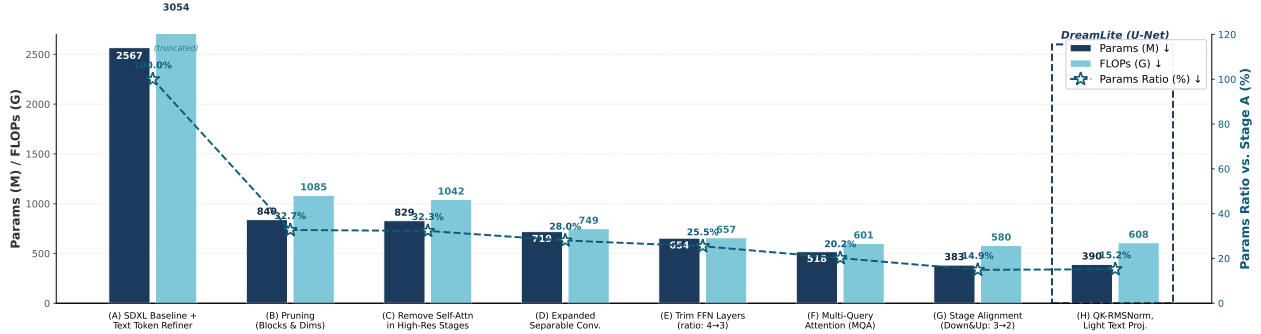


Figure 3 Architectural evolution of DreamLite. We calculate the Parameters (Params) and GFLOPs of the U-Net.

2.5M parameters for image tokenization. It maps image x as a 4-channel latent z with an 8×8 downsampling factor, facilitating efficient training and inference.

Compact UNet. Efficiency is the primary objective guiding the design of DreamLite. To this end, we build upon the mobile-efficient T2I architecture of SnapGen [17], a systematically compressed version of SDXL [39]. Specifically, we optimized the U-Net backbone by making it both shallower and thinner: the number of transformer blocks was reduced from [0, 2, 10] to [0, 2, 4], and the channel dimensions were shrunk from [320, 640, 1280] to [256, 512, 896] and a latent sample size is 128×128 . We further enhanced efficiency through several key optimizations:

- Remove self-attention layers at high-resolution stages to mitigate quadratic complexity;
- Replace standard convolutions with expanded separable convolutions (*i.e.*, depthwise convolution & pointwise convolution);
- Set the hidden channel expansion ratio to 3 in the feed-forward network.
- Adopt Multi-Query Attention (MQA) with a single KV head to reduce both computational overhead and memory footprint;
- Stage alignment, add QK-RMSNorm and a light text projector.

As summarized in Fig. 3, this step-by-step optimization successfully compresses the 2.5B baseline into a highly efficient 389M parameter backbone, significantly reducing FLOPs while preserving generative performance. Additional architectural details can be found in the original SnapGen paper [17].

Text Encoder. For text conditioning, we utilize Qwen3-VL-2B [3] as our text encoder. We leverage its robust visual-language comprehension capabilities to accurately interpret complex user instructions and process multimodal inputs. This choice ensures precise semantic alignment between the input instructions and the generated content.

In-context Paradigm. Existing UNet-based image editing methods [4, 13, 20] typically follow the Instruct-Pix2Pix paradigm [4], which concatenates the condition image with the noisy latent in the channel dimension and fine-tunes the model. However, this mechanism inevitably degrades the generative priors of the pretrained text-to-image (T2I) model and hinders the development of a unified architecture. To address these limitations, we propose extending the UNet with an in-context conditioning framework that unifies both image generation and editing tasks at the input level within a single compact network. As shown in Fig. 2, we construct a two-panel latent by concatenating the latent of the target image (z_{tgt}) and the conditioning image z_{cond} along the width (spatial) dimension:

$$z^{\text{pair}} = \text{Concat}(z_{\text{tgt}}, z_{\text{cond}}), \quad (1)$$

where the left panel corresponds to the target output and the right panel provides the visual condition. The concatenated latent z^{pair} is fed directly into the U-Net. For text-to-image generation, we set the conditioning panel to a blank (all-black) image x_{blank} (with latent z_{blank}) to represent “no visual condition”. For image editing, we use the source image x_{src} (latent z_{src}) as the condition. This design allows the model to extend

from T2I to editing directly without introducing additional modules, making it highly suitable for a unified framework. To further reduce task ambiguity when training a single model for two behaviors, we prepend explicit task tokens to the text prompt: **[Generate]** for generation task and **[Edit]** for editing task. These tokens act as lightweight routing signals without requiring extra parameters or task-specific branches, thereby improving both generation quality and edit controllability under a unified framework. We also compare this in-context formulation with InstructPix2Pix; further details and motivation regarding the architectural design are provided in Section 4.

3.2 Task-progressive Joint Pretraining

Training a compact model with a unified formulation is challenging due to its limited capacity and the divergent optimization objectives of generation and editing tasks. To ensure stable convergence, we propose a task-progressive joint pretraining scheme. Unlike standard approaches that transition directly from text-to-image pretraining to joint training, we introduce an intermediate editing pretraining stage. This stage serves to align the visual conditioning representations with the generative latent space before the complex joint optimization, thereby mitigating task interference. Specifically, the pretraining of DreamLite is divided into three progressive stages: (i) T2I Pretraining, (ii) Editing Training, and (iii) Unified Joint Training.

3.2.1 Text-to-Image Pretraining

We first train the DreamLite as a standard text-to-image diffusion model using the flow matching objective [29, 32]. During training, the noisy latent z_t is constructed through linear interpolation between the initial Gaussian noise ϵ and the clean image latent z , *i.e.*, $z_t = F(z, t) = t \cdot z + (1 - t) \cdot \epsilon$ and $t \in [0, 1]$. The model is then trained to predict the velocity of the vector field that defines the trajectory between the noise and data distributions, *i.e.*, $v_t = z - \epsilon$. The training objective can be formulated as:

$$\mathcal{L}_{\text{fm}} = \mathbb{E}_{t,z,\epsilon,y} [\|v_\theta(z_t, t, y) - (z - \epsilon)\|^2], \quad (2)$$

where v_θ denotes the denoising UNet, θ represents the learnable parameters and y denotes the conditional embeddings. To improve convergence and stability, we adopt a progressive resolution curriculum following prior work [17]. The training proceeds sequentially from 256×256 to 512×512 , and finally to 1024×1024 resolution, with a multi-scale training strategy applied at each stage. Furthermore, following Stable Diffusion 3 [11], we employ a logit-normal noise sampler to concentrate training on intermediate timesteps. We also utilize dynamic time shifting [23] to scale noise levels according to image resolution. Collectively, this stage establishes a strong generative prior for subsequent training stages.

3.2.2 Edit Pretraining

Following T2I pretraining, we activate the in-context conditioning mechanism and continue training the model on paired text-guided image editing data. The primary objective of this stage is to align the newly introduced visual conditioning with the pre-trained generative latent space, enabling the model to generate images based on both condition images and editing instructions. We also employ a flow-matching loss during this phase. However, a major challenge in training for editing tasks is that the target edit regions in the target images are usually small. If a standard uniform loss is applied to the entire image, the gradient signal from these small edited regions can be overwhelmed by the dominant signal from the unchanged background, leading to unsatisfactory editing results. To mitigate this imbalance, following UniWorld-V1 [28], we apply a foreground-emphasis mask to re-weight the loss. Concretely, for localized editing tasks, we derive the edited region mask through a four-step pipeline:

- Pixel-wise Differencing: we compute the absolute difference between source and target images, applying a tolerance threshold to identify candidate regions;
- Dilation: a dilation operator is applied to reduce pixel-level noise;
- Connected Component Filtering: we filter out small, isolated components to eliminate spurious artifacts;
- Max-pooling Downsampling: max-pooling is utilized to remove internal noise within connected regions and we estimate the edited area size A_{edit} .

To prevent small edited regions from being overwhelmed by the static background, we assign higher loss weights to the masked pixels based on the area ratio $x = A_{\text{total}}/A_{\text{edit}}$, where A_{total} denotes the full image area. Subsequently, we use a logarithmic weighting function $w(x) = \log_2(x) + 1$ to balance training stability with sensitivity to minor edits. This mask strategy is applied exclusively to local editing; for global editing or style transfer, we maintain uniform weighting to preserve global distribution alignment.

Finally, we compute this weighting mask w to applied to the flow matching objective:

$$\mathcal{L}_{\text{fmw}} = \mathbb{E}_{t,z,\epsilon,y} [\|w \odot (v_\theta(z_t, t, y) - w \odot (z - \epsilon))\|^2]. \quad (3)$$

Intuitively, the mask focuses the learning signal on regions that differ between source and target images, encouraging the model to make stronger, more faithful edits while preserving the unchanged background.

3.2.3 Unified Pretraining

Subsequently, we perform unified joint training on a mixture of T2I and editing data. This stage is designed to consolidate the generative priors established in the T2I stage with the instruction-following capabilities acquired during Edit pretraining, ensuring the model converges to a single set of parameters that reliably supports both behaviors. As stated in Sec. 3.1, to mitigate task conflict in this unified setting, we prepend explicit task tokens to the text prompts: **[Generate]** to indicate the absence of a visual reference for generation tasks, and **[Edit]** for editing instructions. These tokens function as lightweight routing signals, guiding the model to switch behaviors dynamically based on the input context. Consequently, DreamLite achieves robust performance in both generation and editing under a strictly unified architecture, eliminating the need for additional parameters.

3.3 Post Training

While our task-progressive joint pretraining establishes a strong foundation for both generation and editing, the model’s behavior remains unstable due to the high variance of the pretraining data. To improve stability and performance, we employ a two-stage post-training strategy: Supervised Fine-Tuning (SFT) and Reinforcement Learning (RL).

3.3.1 Supervised Fine-Tuning (SFT).

The primary goal of SFT is to refine the model’s behavior by exposing it to a curated distribution of high-quality data. To achieve this, we construct a dataset comprising approximately 0.5M samples, selected for their high visual quality and caption diversity. By fine-tuning on these cleaner, denser signals, we effectively steer the model’s target distribution toward a manifold of higher realism and precise instruction following.

3.3.2 Reinforcement Learning (RL).

To further align DreamLite with human preferences, we incorporate Reinforcement Learning from Human Feedback (RLHF). Specifically, we adopt the Reward Feedback Learning (ReFL) framework [56], which directly leverages scalar signals from a pre-trained reward model to guide the denoising trajectory via gradient backpropagation. During training, given a condition c and a timestep t , the model progressively denoises the latent to time t to predict the corresponding clean image \hat{x} . A scalar reward $r(c, \hat{x})$ is then computed using the reward model, and gradients are backpropagated through the denoising process. We adopt a ReLU-truncated reward formulation:

$$\mathcal{L}_{\text{rl}} = -\max(0, r(c, \hat{x}) - b), \quad (4)$$

where b is a hyperparameter introduced to ensure training stability and mitigate reward hacking. In our experiments, we employ task-specific reward models to optimize distinct capabilities. For text-to-image generation, we utilize HPSv3 [36], a state-of-the-art preference model built upon the Qwen-VL backbone, with $b = 11$. For image editing, we employ EditReward [53], which is explicitly designed to evaluate adherence to editing instructions, and use $b = 2.5$. This post-training stage consistently enhances both perceptual quality and instruction following, enabling our compact model to outperform prior mobile diffusion baselines.

Category	Source / Content Type	Samples
<i>Part A: Generation Data (20.0M)</i>		
General Perception	COYO, LAION, JoourneyDB, <i>etc.</i>	14.8M
Human & Portrait	High-quality human, Portrait subsets	0.4M
Graphic Design	Text content, Canva subsets	0.4M
Scene Text	Dense/Large scene text	1.5M
Artistic Styles	Midjourney style prompts	0.6M
Specialized Prompts	Object relations, Text rendering	2.4M
<i>Part B: Editing Data (1.74M)</i>		
Understanding	Feature Extraction & Parsing, Action	429k
Local Edit	Add, Remove, Color, Replace, <i>etc.</i>	830k
Global Edit	Enhance, Lighting, Background	300k
View Edit	Camera View, Zoom In/Out, Outpainting	151k
Style Edit	Unreal ↔ Real	31k

Table 1 Detailed distribution of the 21.7M total samples.

3.4 Step Distillation

While our post-training strategy ensures high-quality generation, it still requires tens of denoising steps to generate/edit an image, creating a significant bottleneck for real-time mobile applications. To bridge the gap between high-fidelity synthesis and low-latency deployment, we apply Distribution Matching Distillation (DMD) [59, 60] to reduce the sampling process to just 4 steps without compromising visual quality. DMD distills a multi-step diffusion teacher into a few-step generator G by minimizing the approximate Kullback-Leibler (KL) divergence between the distribution of real images $p_{\text{real},t}$ and the generator’s output distribution $p_{\text{fake},t}$. The gradient of DMD loss is computed as:

$$\begin{aligned} \nabla \mathcal{L}_{\text{DMD}} &= \mathbb{E}_t (\nabla_{\theta} \text{KL}(p_{\text{fake},t} \| p_{\text{real},t})) \\ &= -\mathbb{E}_t \left(\int (s_{\text{real}}(F(G_{\theta}(\epsilon), t), t) - s_{\text{fake}}(F(G_{\theta}(\epsilon), t), t)) \frac{dG_{\theta}(\epsilon)}{d\theta} d\epsilon \right), \end{aligned} \quad (5)$$

where $\epsilon \sim \mathcal{N}(0, \mathbf{I})$ is a random Gaussian noise, and θ denotes the generator parameters. F defines the forward diffusion process that transfers the generated sample $G_{\theta}(\epsilon)$ the noise level corresponding to timestep t . s_{real} and s_{fake} represent the scores, approximated using diffusion models v_{real} and v_{fake} , respectively. To stabilize training, we also employ the GAN loss \mathcal{L}_{GAN} [59] to enhance the diversity and realism of the generated images for the distilled model. Our distilled model enables high-quality image generation and editing in only 4 sampling steps without the need for CFG, showcasing exceptional efficiency.

4 Experiments

4.1 Implementation Details

DreamLite is implemented using the PyTorch. The training corpus consists of 20M text-to-image pairs and 1.7M image editing samples. During the unified joint training stage, we employ a sampling ratio of approximately 1:1 between T2I and editing data to balance performance. We utilize the AdamW optimizer with a staged learning rate schedule: 1×10^{-4} for initial T2I pre-training, 1×10^{-5} for editing training and 1×10^{-6} for unified joint training. The batch size is set to 576.

4.2 Dataset Information

Text-to-image Generation Dataset. To establish a robust and diverse generative prior, our text-to-image (T2I) pre-training utilizes a curated corpus of approximately 20M samples. We categorize these data into five primary domains: General Perception, Human & Portrait, Graphic Design, Scene Text, and Artistic Styles. Specifically, we leverage large-scale open-source datasets (*e.g.*, LAION [43], COYO [5], JourneyDB [47]) for general semantic alignment, while incorporating specialized subsets for high-quality human generation and

Model	Param.	Single Obj.	Two Obj.	Counting	Colors	Position	Color Attr.	Overall
FLUX.1-Dev [23]	12B	0.99	0.81	0.79	0.74	0.20	0.47	0.67
BAGEL [10]	7B	0.99	0.94	0.81	0.88	0.64	0.63	0.82
OmniGen2 [52]	4B	1.00	0.95	0.64	0.88	0.55	0.76	0.80
Z-Image [6]	6B	1.00	0.94	0.78	0.93	0.62	0.77	0.84
LongCat-Image [48]	6B	0.99	0.98	0.86	0.86	0.75	0.73	0.87
DeepGen1.0 [50]	2B	0.99	0.97	0.68	0.90	0.71	0.71	0.83
SANA-1.6B [55]	1.6B	0.99	0.80	0.62	0.89	0.27	0.43	0.67
Hunyuan-DiT [7]	1.5B	0.97	0.77	0.71	0.88	0.13	0.30	0.63
MEISSONIC [2]	1B	0.99	0.66	0.42	0.86	0.10	0.22	0.54
SnapGen [17]	0.38B	-	-	-	-	-	-	0.70
SnapGen++ [18]	0.4B	-	-	-	-	-	-	0.66
SANA-0.6B [55]	0.59B	0.98	0.78	0.59	0.86	0.22	0.40	0.64
Nitro-E-GRPO [46]	0.3B	1.00	0.88	0.63	0.86	0.32	0.48	0.70
Ours	0.39B	0.98	0.88	0.65	0.90	0.35	0.52	0.72

Table 2 Evaluation on GenEval benchmark. All images are generated at 1024×1024 resolution. “Param.” denotes backbone parameters.

complex text rendering. For all samples, we prioritize high-resolution images and apply a stringent filtering pipeline to remove low-quality captions samples. The data composition is summarized in Table 1.

Image Editing Dataset. To empower DreamLite with comprehensive instruction-following capabilities, we curated an image editing corpus comprising approximately 1.7M samples. These samples are categorized into five primary groups:

- **Understanding Edit:** A significant portion of the data is for editing-oriented understanding such as feature extraction and human action adjustments (*e.g.*, age, expression, pose).
- **Local Edit:** This includes fine-grained modifications such as object addition/removal and color/material changes, *etc.*
- **Global Edit:** This category focuses on overall image enhancements, including lighting direction adjustments, background modifications, *etc.*
- **View Edit:** It involves spatial and structural transformations, such as camera view adjustments, zooming (in/out) and object-level rotation or motion.
- **Style Edit:** This one mainly focus on style transfer (unreal-to-real).

The detailed data distribution across these fine-grained categories is presented in Table 1.

4.3 Quantitative Results

To evaluate the performance of DreamLite, we conduct extensive comparative experiments across multiple mainstream benchmarks, focusing on both Image Editing and Image Generation capabilities.

Performance on Image Generation. We first assess the generative quality using GenEval [14] and DPG [19] as the primary benchmarks with all images generated at 1024×1024 resolution for a fair comparison. The compared baselines are categorized into three groups:

- **Unified Models** (*e.g.*, BAGEL, OmniGen2), which typically feature backbone sizes exceeding 2B parameters;
- **Lightweight Generative Models ($< 2B$)** (*e.g.*, SANA-1.6B, Meissonic), which remain unsuitable for seamless on-device deployment;
- **On-device Generative Models ($< 1B$)** (*e.g.*, SnapGen series, SANA-0.6B), which are restricted to only generation tasks.

Model	Param.	Global	Entity	Attribute	Relation	Other	Overall
FLUX.1-Dev [23]	12B	82.1	89.5	88.7	91.1	89.4	84.0
BAGEL [10]	7B	88.9	90.4	91.3	90.8	88.7	85.1
OmniGen2 [52]	4B	88.8	88.8	90.2	89.4	90.3	83.6
Z-Image [6]	6B	93.4	91.2	93.2	92.2	91.5	88.1
LongCat-Image [48]	6B	89.1	92.5	92.0	93.3	87.5	86.6
DeepGen1.0 [50]	2B	84.2	91.0	88.6	94.0	85.3	84.6
SANA-1.6B [55]	1.6B	86.0	91.5	88.9	91.9	90.7	84.8
Hunyuan-DiT [7]	1.5B	84.6	80.6	88.0	74.4	86.4	78.9
MEISSONIC [2]	1B	75.8	74.3	74.4	81.5	57.6	65.3
SnapGen [17]	0.38B	-	-	-	-	-	81.1
SnapGen++ [18]	0.4B	-	-	-	-	-	85.2
SANA-0.6B [55]	0.59B	83.0	89.5	89.3	90.1	90.2	83.6
Nitro-E-GRPO [46]	0.3B	82.7	87.6	86.9	92.1	74.9	81.1
Ours	0.39B	84.9	91.6	89.7	94.3	80.4	85.8

Table 3 Evaluation on DPG benchmark. All images are generated at 1024×1024 resolution. “Param.” denotes backbone parameters.

Model	Param.	Add	Remove	Replace	Adjust	BG	Style	Extract	Action	Hybrid	Overall
Kontext-Dev [25]	12B	4.04	2.92	4.28	3.89	4.00	4.43	2.71	4.52	3.08	3.76
BAGEL [10]	7B	3.81	3.16	3.85	3.59	3.39	4.51	1.58	4.25	2.67	3.42
OmniGen2 [52]	4B	3.57	3.20	3.74	3.06	3.57	4.81	1.77	4.68	2.52	3.44
Z-Image [6]	6B	4.40	4.13	4.57	4.14	4.14	4.85	4.30	4.50	3.63	4.30
LongCat-Image [48]	6B	4.66	4.68	4.75	4.64	4.35	4.81	3.90	4.83	3.80	4.49
DeepGen1.0 [50]	2B	4.52	4.43	4.42	4.09	4.38	4.48	1.75	4.57	3.61	4.03
VIBE [1]	1.6B	3.89	4.42	4.34	4.22	4.22	4.40	2.90	2.75	3.52	3.85
EditMGT [9]	0.96B	2.78	2.89	3.34	3.29	3.05	4.17	1.56	2.94	2.01	2.89
Ours	0.39B	4.59	4.27	4.32	4.46	4.28	4.42	2.70	4.73	3.24	4.11

Table 4 Evaluation on ImgEdit benchmark. “Param.” denotes backbone parameters.

Table 2 and Table 3 details the parameter counts, per-category scores and overall performance on GenEval and DPG benchmark. Note that for the SnapGen series, per-category scores are omitted as the models are not open-sourced. Nevertheless, DreamLite (0.39B) achieves competitive performance, rivaling models with nearly $10\times$ more parameters.

Performance on Image Editing. We evaluate editing proficiency using the ImgEdit [58] and GEdit [31] benchmarks. For ImgEdit, we employ GPT-4o (2024-11-20) as the automated evaluation metric. For GEdit, we focus on English-based editing tasks and utilize Qwen2.5-VL [3] as the model-based judge. Similar to generation task, our method is compared against a broad spectrum of state-of-the-art (SOTA) baselines, categorized into:

- Unified Models (*e.g.*, FLUX, BAGEL, LongCat-Image);
- Lightweight Editing Models ($< 2B$) (*i.e.*, VIBE);
- On-device Editing Models ($< 1B$) (*i.e.*, EditMGT).

Crucially, to the best of our knowledge, DreamLite is among the first to successfully enable image editing tasks on-device with a model scale significantly under 0.5B parameters. Table 4 summarizes the model sizes, per-category scores and overall performance on the ImgEdit benchmark. DreamLite achieves SOTA among all lightweight models.

Model	Param.	Q_{SC}	Q_{PQ}	Q_O
Kontext-Dev [25]	12B	6.61	7.24	6.79
BAGEL [10]	7B	7.66	7.08	7.20
OmniGen2 [52]	4B	7.11	7.22	6.79
LongCat-Image [48]	6B	7.87	7.49	7.55
DeepGen1.0 [50]	2B	7.83	7.47	7.54
VIBE [1]	1.6B	7.61	7.34	7.28
EditMGT [9]	0.96B	6.77	6.74	6.33
Ours	0.39B	7.04	7.54	6.88

Table 5 Evaluation on GEdit-EN benchmark. “Param.” denotes backbone parameters. Q_{SC} , Q_{PQ} , and Q_O denote Semantic Consistency, Perceptual Quality and Overall score evaluated by Qwen-VL-2.5 respectively.

4.4 Qualitative Results

To further validate the visual fidelity and instruction-following capability of our DreamLite, we present a qualitative comparison with both large unified models and specialized lightweight baselines.

Visual Analysis of Image Generation. As illustrated in Fig. 4, although DreamLite is significantly smaller than other large-scale models, it maintains high structural integrity and strong semantic alignment across diverse generation scenarios. For instance, in complex realistic prompts such as “A rain-soaked street at dawn...”, DreamLite accurately captures the atmospheric lighting and produces consistent structural details of the “bicycle”, avoiding the distortion often seen in smaller counterparts. Furthermore, in stylized and imaginative generation tasks, ranging from a “Cute isometric 3D icon of a pastel mint green cactus in clay texture” to a “Whimsical children’s storybook illustration” featuring multiple subjects (a horse and an oversized black cat), our model demonstrates a profound understanding of stylistic nuances and complex spatial compositions. Compared to other lightweight models like Nitro-E (0.3B) or Meissonic (1B), our results consistently exhibit superior scene composition, better adherence to stylistic constraints (*e.g.*, clay animation-style or stylized digital blooms), and significantly fewer artifacts in high-resolution synthesis. While there might be a marginal gap in rendering extremely fine-grained textures in human portraits when compared to larger specialized models like SANA-1.6B, our model provides a more robust and coherent interpretation of environmental lighting, mood, and complex multi-object interactions (*e.g.*, “A small French bulldog puppy sitting at a café table... looking at a croissant”).

Visual Analysis of Image Editing. The image editing comparisons in Fig. 5 further highlight the performance of DreamLite. For instance, in object addition and removal tasks (*e.g.*, “Place a bicycle in the foreground of the flower field” or “Remove the white baby onesie from the image”), our model demonstrates a precise understanding of spatial relationships and occlusion comparable to large-scale models (*e.g.*, OmniGen2 and BAGEL). Furthermore, when dealing with complex style and background transformations (*e.g.*, “Transfer the image into a hand-sculpted claymation style” or “Change the background from a clear blue sky with bare branches to a sunset sky over a lush forest”), our approach successfully preserves the structural integrity of the main subjects while seamlessly applying the desired modifications. In addition, for fine-grained localized edits, such as texture alterations and multi-object manipulation (*e.g.*, “Change the tortoise’s shell texture to a smooth surface” or “Remove the basket of fruit on the coffee table, and change the color of the left armchair cushion to dark green”), our model efficiently executes intricate instructions without unintended disruptions to the surrounding context, proving its high instruction-following capability despite having significantly fewer parameters (0.39B) compared to models like Kontext (12B) or LongCat (6B).

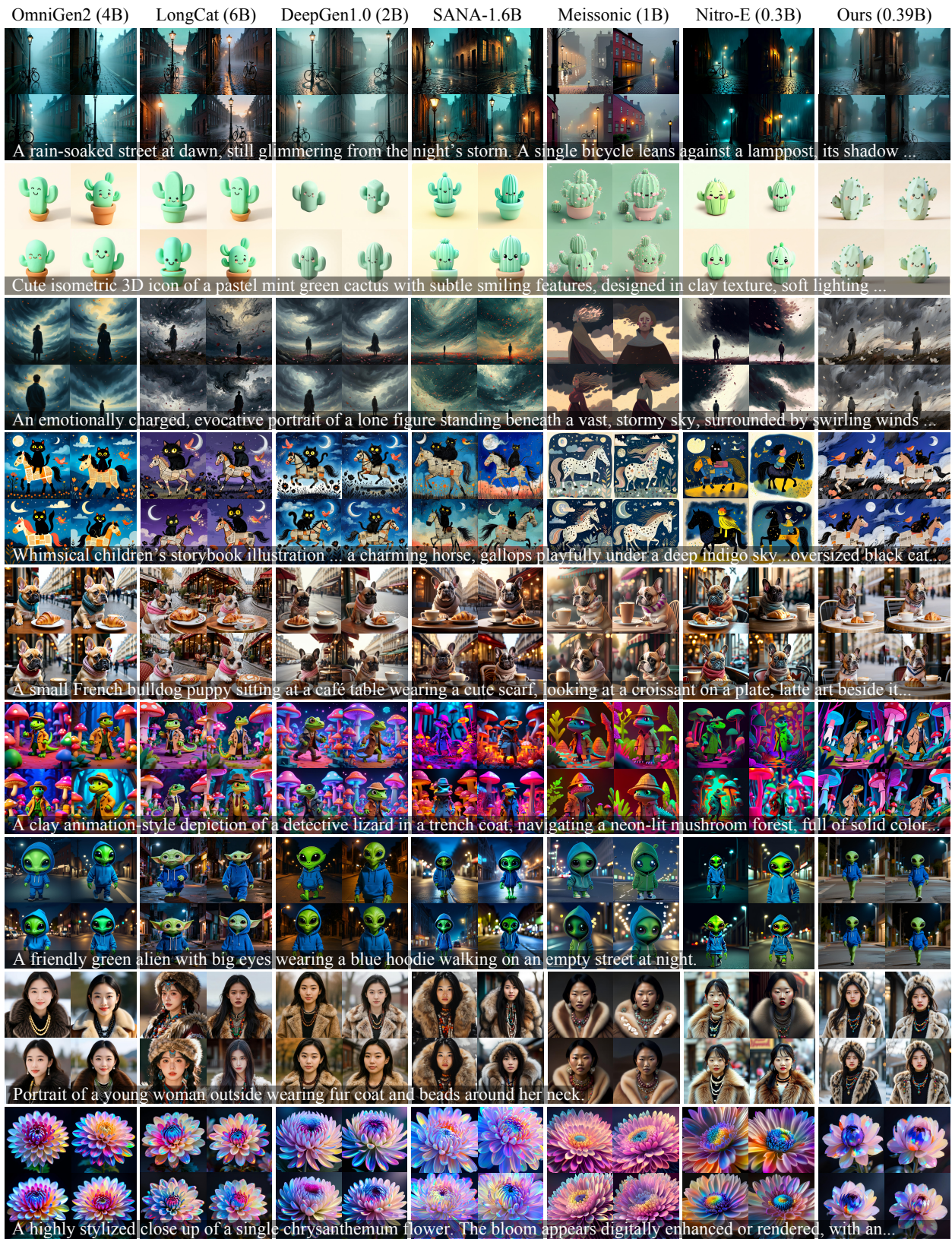


Figure 4 Comparison of image generation. All input prompts are listed at the bottom of the images.

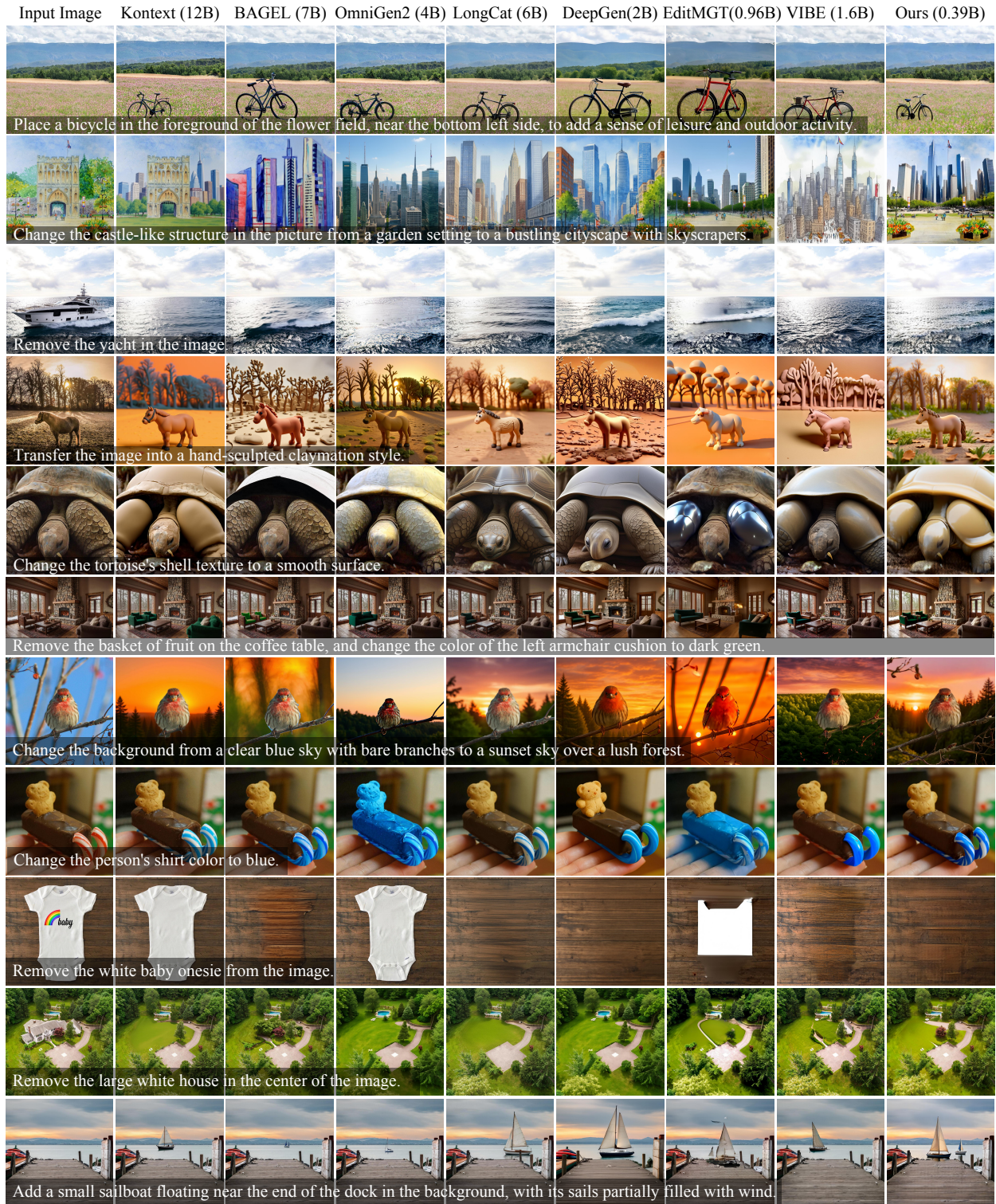


Figure 5 Comparison of image editing. All source images and instructions are from ImgEdit Benchmark.

Exp.	Mechanism	Training Stage	GenEval \uparrow	ImgEdit \uparrow
Text-to-image Pretraining			0.70	-
Condition Mechanism	Pix2Pix	T2I \rightarrow Edit	0.56	3.67
	Pix2Pix	T2I \rightarrow Edit \rightarrow Unified	0.61	3.65
Training Recipe	In-context	T2I \rightarrow T2I	0.65	-
	In-context	T2I \rightarrow Edit	0.64	3.88
	In-context	T2I \rightarrow Unified	0.65	3.14
	In-context	T2I \rightarrow Edit \rightarrow Unified	0.71	3.94
Reinforcement Learning	In-context	TPJ Pretrain \rightarrow RLHF	0.72	4.11
Step Distillation	In-context	TPJ Pretrain \rightarrow RLHF \rightarrow DMD	0.70	3.8

Table 6 Ablation study on GenEval and ImgEdit benchmarks. “TPJ” denotes “Task-progressive Joint”.



Figure 6 Ablation study on generation (left) and editing (right) tasks. From left to right in each task: results without RL, our full model, and our model after 4-step distillation.

4.5 Ablation Study

To dissect the contribution of our proposed training strategies, we conduct an extensive ablation study on DreamLite, evaluating generation and editing performance on GenEval and ImgEdit benchmarks. The quantitative results are summarized in Table 6 and the qualitative results are shown in Fig. 6.

Condition Mechanism. We first investigate the effectiveness of the In-context (IC) mechanism compared to the traditional Pix2Pix-style channel concatenation after Text-to-image pretraining. As shown in Table 6, when maintaining the same editing training stage (*i.e.*, T2I \rightarrow Edit, row 2&5), the IC mechanism yields a significant improvement from 3.67 to 3.88. Furthermore, compared to the results at unified training stage (*i.e.*, T2I \rightarrow Edit \rightarrow Unified, row 3&7), the IC mechanism proves more suitable for joint training, particularly for the generation task (from 0.61 to 0.71). We attribute this to the fact that IC treats the generation as a special case of in-context referencing (*i.e.*, the condition image is represented by a blank image). This formulation allows the model to leverage a unified spatial prior across disparate behaviors.

Training Recipe. The transition from specialized tasks to unified behavior often encounters a performance bottleneck. Our results indicate that direct joint training (*i.e.*, T2I \rightarrow Unified, row 6) sacrifices both generation and editing precision simultaneously (*e.g.*, GenEval 0.65 and ImgEdit 3.14). By introducing Task-progressive Joint (TPJ) Pre-training (*i.e.*, T2I \rightarrow Edit \rightarrow Unified, row 7), we observe that the model not only recovers but also surpasses the performance of separate tasks (GenEval 0.71 *vs.* 0.70 and ImgEdit 3.91 *vs.* 3.88). This demonstrates that TPJ allows the compact backbone to internalize the fundamental logic of IC referencing before tackling unified modeling. We also conduct in-context T2I training following standard T2I pre-training (row 4), which results in a slight decline in GenEval performance. We posit that since the blank image provides no information, the model fails to utilize it for contextual referencing, thereby slowing down convergence and compromising T2I performance.

Reinforcement Learning. As shown in Table 6, integrating RLHF into the TPJ pipeline yields the highest

overall performance, achieving 4.11 on ImgEdit and 0.72 on GenEval. Beyond these numerical gains, visual evidence in Fig. 6 demonstrates a substantial leap in image aesthetics and high-frequency details. Specifically, it markedly improves background realism in generation tasks and enhances human identity maintenance during editing.

Step Distillation. DMD significantly accelerates the sampling process, albeit with a slight performance penalty in complex semantic alignment tasks. Fig. 6 presents the visual results of DreamLite with 4-step inference after Distribution Matching Distillation. This performance-efficiency trade-off is expected, as the compression of the ODE trajectory inherently constrains the model’s capacity to navigate high-dimensional latent manifolds for intricate edits.

4.6 On-device Deployment



Figure 7 DreamLite generation and editing examples on mobile device.

To evaluate the practical utility of DreamLite, we conduct comprehensive experiments on real mobile phones (*i.e.*, Xiaomi 14 and vivo X100), equipped with the Snapdragon 8 Gen3 (Qualcomm NPU) and Dimensity 9300 (MTK APU). All measurements are performed using a quantized W8A8 (*i.e.*, weights 8-bit, activations 8-bit) U-Net backbone at a 1024×1024 resolution with a 4-step sampling schedule.

Runtime Optimization. Given that the standard Qwen3-VL text encoder comprises approximately 2B parameters, direct on-device text encoding remains a primary latency bottleneck. We choose to pre-deploy common prompts (*e.g.*, stylized or predefined editing tasks) as pre-computed embeddings for instantaneous interaction on mobile devices. For future iterations, we are developing a lightweight text encoder (<1B) to enable full-pipeline on-device flexibility without compromising inference speed.

Performance Analysis. As summarized in Table 7, the U-Net inference per step is merely 103.84ms on the Snapdragon 8 Gen3, leading to a total generation or editing time of approximately 0.42s (excluding VAE). Including VAE decoding (~ 22 ms) and system overhead, the end-to-end user experience remains near the 1s threshold. Fig. 7 shows our generation (left) and editing (right) results. The UNet is quantized as W8A8 with a 4-step inference.

Component	Snapdragon 8 Gen3	Dimensity 9300	Model Size
VAE Encoder (fp16)	22.17	26.16	2.45 MB
U-Net (w8a8, per step)	103.84	122.53	389.00 MB
VAE Decoder (fp16)	22.17	26.16	2.45 MB
Total (4 steps, U-Net)	415.36	490.12	393.90 MB

Table 7 On-device inference latency (ms) for DreamLite components at 1024×1024 resolution. Measurements are conducted on W8A8 quantized models.

5 Limitations

Despite the efficiency and versatility of DreamLite, several limitations remain that define our future research directions.

Text Encoder Scale. Although our U-Net backbone is highly compact (0.39B), the current pipeline still relies on a standard 2B-parameter text encoder. During on-device deployment, this component introduces non-negligible latency. To achieve a fully optimized on-device pipeline, we are actively developing a lightweight text encoder (<1B) to ensure seamless end-to-end inference.

Reconstruction Fidelity and Specialized Tasks. While DreamLite performs competitively on major benchmarks, we observe relatively lower scores on GEdit and certain qualitative artifacts in challenging scenarios (*i.e.*, text generation, text editing and identity preservation in portrait editing). We attribute these bottlenecks to our extremely compact VAE (1.2M), which may inevitably suffer from information loss or reconstruction blurriness when handling complex structural details. To mitigate this, we plan to train a slightly larger, high-fidelity VAE. Furthermore, we are going to implement specialized fine-tuning for text and facial generation or editing to enhance perceptual quality and instruction following.

Multi-modal Alignment. Future work will also explore a more advanced step distillation scheme combined with reward model during the post training stage to better align our compact model with human aesthetic preferences and complex spatial instructions.

6 Conclusion

We presented DreamLite, a compact unified on-device diffusion model that supports both text-to-image generation and text-guided image editing within a single network. By unifying conditioning through in-context spatial concatenation and explicit task tokens, DreamLite achieves seamless multi-tasking without parameter overhead. To stably train this small-capacity unified model, we introduced a task-progressive curriculum (T2I \rightarrow Edit \rightarrow Joint) followed by high-quality SFT and reinforcement learning. Finally, step distillation compresses sampling to 4 denoising steps for efficient mobile inference. Experiments show that DreamLite (GenEval 0.72, ImgEdit 4.11) significantly outperforms prior on-device baselines and remains competitive with much larger server-side model. On representative smartphone (*i.e.*, Xiaomi 14), DreamLite could generate or edit a 1024×1024 image in less than 1s.

References

- [1] Grigori Alekseenko, Aleksandr Gordeev, Irina Tolstykh, Bulat Suleimanov, Vladimir Dokholyan, Georgii Fedorov, Sergey Yakubson, Aleksandra Tsybina, Mikhail Chernyshov, and Maksim Kuprashevich. Vibe: Visual instruction based editor. *arXiv preprint arXiv:2601.02242*, 2026.
- [2] Jinbin Bai, Tian Ye, Wei Chow, Enxin Song, Qing-Guo Chen, Xiangtai Li, Zhen Dong, Lei Zhu, and Shuicheng Yan. Meissonic: Revitalizing masked generative transformers for efficient high-resolution text-to-image synthesis. In *The Thirteenth International Conference on Learning Representations*, 2024.
- [3] Shuai Bai, Yuxuan Cai, Ruizhe Chen, Keqin Chen, Xionghui Chen, Zesen Cheng, Lianghao Deng, Wei Ding, Chang Gao, Chunjiang Ge, et al. Qwen3-vl technical report. *arXiv preprint arXiv:2511.21631*, 2025.
- [4] Tim Brooks, Aleksander Holynski, and Alexei A Efros. Instructpix2pix: Learning to follow image editing instructions. In *Proceedings of the IEEE/CVF conference on computer vision and pattern recognition*, pages 18392–18402, 2023.
- [5] Minwoo Byeon, Beomhee Park, Haecheon Kim, Sungjun Lee, Woonhyuk Baek, and Saehoon Kim. Coyo-700m: Image-text pair dataset. <https://github.com/kakaobrain/coyo-dataset>, 2022.
- [6] Huanqia Cai, Sihan Cao, Ruoyi Du, Peng Gao, Steven Hoi, Zhaohui Hou, Shijie Huang, Dengyang Jiang, Xin Jin, Liangchen Li, et al. Z-image: An efficient image generation foundation model with single-stream diffusion transformer. *arXiv preprint arXiv:2511.22699*, 2025.
- [7] Siyu Cao, Hangting Chen, Peng Chen, Yiji Cheng, Yutao Cui, Xincheng Deng, Ying Dong, Kipper Gong, Tianpeng Gu, Xiuse Gu, et al. Hunyuanimage 3.0 technical report. *arXiv preprint arXiv:2509.23951*, 2025.
- [8] Junsong Chen, Chongjian Ge, Enze Xie, Yue Wu, Lewei Yao, Xiaozhe Ren, Zhongdao Wang, Ping Luo, Huchuan Lu, and Zhenguo Li. Pixart- σ : Weak-to-strong training of diffusion transformer for 4k text-to-image generation. In *European Conference on Computer Vision*, pages 74–91. Springer, 2024.
- [9] Wei Chow, Linfeng Li, Lingdong Kong, Zefeng Li, Qi Xu, Hang Song, Tian Ye, Xian Wang, Jinbin Bai, Shilin Xu, et al. Editmgt: Unleashing potentials of masked generative transformers in image editing. *arXiv preprint arXiv:2512.11715*, 2025.
- [10] Chaorui Deng, Deyao Zhu, Kunchang Li, Chenhui Gou, Feng Li, Zeyu Wang, Shu Zhong, Weihao Yu, Xiaonan Nie, Ziang Song, Guang Shi, and Haoqi Fan. Emerging properties in unified multimodal pretraining. *arXiv preprint arXiv:2505.14683*, 2025.
- [11] Patrick Esser, Sumith Kulal, Andreas Blattmann, Rahim Entezari, Jonas Müller, Harry Saini, Yam Levi, Dominik Lorenz, Axel Sauer, Frederic Boesel, et al. Scaling rectified flow transformers for high-resolution image synthesis. In *Forty-first international conference on machine learning*, 2024.
- [12] Yu Gao, Lixue Gong, Qiushan Guo, Xiaoxia Hou, Zhichao Lai, Fanshi Li, Liang Li, Xiaochen Lian, Chao Liao, Liyang Liu, et al. Seedream 3.0 technical report. *arXiv preprint arXiv:2504.11346*, 2025.
- [13] Zigang Geng, Binxin Yang, Tiankai Hang, Chen Li, Shuyang Gu, Ting Zhang, Jianmin Bao, Zheng Zhang, Houqiang Li, Han Hu, et al. Instructdiffusion: A generalist modeling interface for vision tasks. In *Proceedings of the IEEE/CVF Conference on computer vision and pattern recognition*, pages 12709–12720, 2024.
- [14] Dhruva Ghosh, Hannaneh Hajishirzi, and Ludwig Schmidt. Geneval: An object-focused framework for evaluating text-to-image alignment. *Advances in Neural Information Processing Systems*, 36:52132–52152, 2023.
- [15] Lixue Gong, Xiaoxia Hou, Fanshi Li, Liang Li, Xiaochen Lian, Fei Liu, Liyang Liu, Wei Liu, Wei Lu, Yichun Shi, et al. Seedream 2.0: A native chinese-english bilingual image generation foundation model. *arXiv preprint arXiv:2503.07703*, 2025.
- [16] Google. Gemini 2.5 flash. <https://aistudio.google.com/models/gemini-2-5-flash-image>, 2025.
- [17] Dongting Hu, Jierun Chen, Xijie Huang, Huseyin Coskun, Arpit Sahni, Aarush Gupta, Anujraaj Goyal, Dishani Lahiri, Rajesh Singh, Yerlan Idelbayev, et al. Snapgen: Taming high-resolution text-to-image models for mobile devices with efficient architectures and training. *arXiv preprint arXiv:2412.09619*, 2024.
- [18] Dongting Hu, Aarush Gupta, Magzhan Gabidolla, Arpit Sahni, Huseyin Coskun, Yanyu Li, Yerlan Idelbayev, Ahsan Mahmood, Aleksei Lebedev, Dishani Lahiri, et al. Snapgen++: Unleashing diffusion transformers for efficient high-fidelity image generation on edge devices. *arXiv preprint arXiv:2601.08303*, 2026.

- [19] Xiwei Hu, Rui Wang, Yixiao Fang, Bin Fu, Pei Cheng, and Gang Yu. Ella: Equip diffusion models with llm for enhanced semantic alignment. *arXiv preprint arXiv:2403.05135*, 2024.
- [20] Yuzhou Huang, Liangbin Xie, Xintao Wang, Ziyang Yuan, Xiaodong Cun, Yixiao Ge, Jiantao Zhou, Chao Dong, Rui Huang, Ruimao Zhang, et al. Smartedit: Exploring complex instruction-based image editing with multimodal large language models. In *Proceedings of the IEEE/CVF Conference on Computer Vision and Pattern Recognition*, pages 8362–8371, 2024.
- [21] Zhiwei Jia, Yuesong Nan, Huixi Zhao, and Gengdai Liu. Reward fine-tuning two-step diffusion models via learning differentiable latent-space surrogate reward. In *Proceedings of the Computer Vision and Pattern Recognition Conference*, pages 12912–12922, 2025.
- [22] Yuval Kirstain, Adam Polyak, Uriel Singer, Shahbuland Matiana, Joe Penna, and Omer Levy. Pick-a-pic: An open dataset of user preferences for text-to-image generation. *Advances in neural information processing systems*, 36:36652–36663, 2023.
- [23] Black Forest Labs. Flux. <https://github.com/black-forest-labs/flux>, 2024.
- [24] Black Forest Labs. Flux2. <https://github.com/black-forest-labs/flux2>, 2025.
- [25] Black Forest Labs, Stephen Batifol, Andreas Blattmann, Frederic Boesel, Saksham Consul, Cyril Diagne, Tim Dockhorn, Jack English, Zion English, Patrick Esser, et al. Flux. 1 kontext: Flow matching for in-context image generation and editing in latent space. *arXiv preprint arXiv:2506.15742*, 2025.
- [26] Jiachen Li, Weixi Feng, Wenhui Chen, and William Yang Wang. Reward guided latent consistency distillation. *arXiv preprint arXiv:2403.11027*, 2024.
- [27] Yanyu Li, Huan Wang, Qing Jin, Ju Hu, Pavlo Chemerys, Yun Fu, Yanzhi Wang, Sergey Tulyakov, and Jian Ren. Snapfusion: Text-to-image diffusion model on mobile devices within two seconds. *Advances in Neural Information Processing Systems*, 36:20662–20678, 2023.
- [28] Bin Lin, Zongjian Li, Xinhua Cheng, Yuwei Niu, Yang Ye, Xianyi He, Shenghai Yuan, Wangbo Yu, Shaodong Wang, Yunyang Ge, et al. Uniworld-v1: High-resolution semantic encoders for unified visual understanding and generation. *arXiv preprint arXiv:2506.03147*, 2025.
- [29] Yaron Lipman, Ricky TQ Chen, Heli Ben-Hamu, Maximilian Nickel, and Matt Le. Flow matching for generative modeling. *arXiv preprint arXiv:2210.02747*, 2022.
- [30] Jie Liu, Gongye Liu, Jiajun Liang, Yangguang Li, Jiaheng Liu, Xintao Wang, Pengfei Wan, Di Zhang, and Wanli Ouyang. Flow-grpo: Training flow matching models via online rl. *arXiv preprint arXiv:2505.05470*, 2025.
- [31] Shiyu Liu, Yucheng Han, Peng Xing, Fukun Yin, Rui Wang, Wei Cheng, Jiaqi Liao, Yingming Wang, Honghao Fu, Chunrui Han, Guopeng Li, Yuang Peng, Quan Sun, Jingwei Wu, Yan Cai, Zheng Ge, Ranchen Ming, Lei Xia, Xianfang Zeng, Yibo Zhu, Binxing Jiao, Xiangyu Zhang, Gang Yu, and Daxin Jiang. Step1x-edit: A practical framework for general image editing. *arXiv preprint arXiv:2504.17761*, 2025.
- [32] Xingchao Liu, Chengyue Gong, and Qiang Liu. Flow straight and fast: Learning to generate and transfer data with rectified flow. *arXiv preprint arXiv:2209.03003*, 2022.
- [33] Simian Luo, Yiqin Tan, Longbo Huang, Jian Li, and Hang Zhao. Latent consistency models: Synthesizing high-resolution images with few-step inference. *arXiv preprint arXiv:2310.04378*, 2023.
- [34] Weijian Luo. Diff-instruct++: Training one-step text-to-image generator model to align with human preferences. *arXiv preprint arXiv:2410.18881*, 2024.
- [35] Yihong Luo, Tianyang Hu, Weijian Luo, Kenji Kawaguchi, and Jing Tang. Reward-instruct: A reward-centric approach to fast photo-realistic image generation. *arXiv preprint arXiv:2503.13070*, 2025.
- [36] Yuhang Ma, Xiaoshi Wu, Keqiang Sun, and Hongsheng Li. Hpsv3: Towards wide-spectrum human preference score. In *Proceedings of the IEEE/CVF International Conference on Computer Vision*, pages 15086–15095, 2025.
- [37] Madebyollin. taesd. <https://github.com/madebyollin/taesd>, 2024.
- [38] OpenAI. Gpt-image. <https://openai.com/index/gpt-4o-system-card/>, 2025.

- [39] Dustin Podell, Zion English, Kyle Lacey, Andreas Blattmann, Tim Dockhorn, Jonas Müller, Joe Penna, and Robin Rombach. Sdxl: Improving latent diffusion models for high-resolution image synthesis. *arXiv preprint arXiv:2307.01952*, 2023.
- [40] Mihir Prabhudesai, Anirudh Goyal, Deepak Pathak, and Katerina Fragkiadaki. Aligning text-to-image diffusion models with reward backpropagation. 2023.
- [41] Robin Rombach, Andreas Blattmann, Dominik Lorenz, Patrick Esser, and Björn Ommer. High-resolution image synthesis with latent diffusion models. In *Proceedings of the IEEE/CVF conference on computer vision and pattern recognition*, pages 10684–10695, 2022.
- [42] Axel Sauer, Dominik Lorenz, Andreas Blattmann, and Robin Rombach. Adversarial diffusion distillation. In *European Conference on Computer Vision*, pages 87–103. Springer, 2024.
- [43] Christoph Schuhmann, Romain Beaumont, Richard Vencu, Cade Gordon, Ross Wightman, Mehdi Cherti, Theo Coombes, Aarush Katta, Clayton Mullis, Mitchell Wortsman, et al. Laion-5b: An open large-scale dataset for training next generation image-text models. *Advances in neural information processing systems*, 35:25278–25294, 2022.
- [44] Team Seedream, Yumpeng Chen, Yu Gao, Lixue Gong, Meng Guo, Qiushan Guo, Zhiyao Guo, Xiaoxia Hou, Weilin Huang, Yixuan Huang, et al. Seedream 4.0: Toward next-generation multimodal image generation. *arXiv preprint arXiv:2509.20427*, 2025.
- [45] Abdelrahman Shaker, Ahmed Heakl, Jaseel Muhammad, Ritesh Thawkar, Omkar Thawakar, Senmao Li, Hisham Cholakkal, Ian Reid, Eric P Xing, Salman Khan, et al. Mobile-o: Unified multimodal understanding and generation on mobile device. *arXiv preprint arXiv:2602.20161*, 2026.
- [46] Tong Shen, Jingai Yu, Dong Zhou, Dong Li, and Emad Barsoum. E-mmdit: Revisiting multimodal diffusion transformer design for fast image synthesis under limited resources. *arXiv preprint arXiv:2510.27135*, 2025.
- [47] Keqiang Sun, Junting Pan, Yuying Ge, Hao Li, Haodong Duan, Xiaoshi Wu, Renrui Zhang, Aojun Zhou, Zipeng Qin, Yi Wang, et al. Journeydb: A benchmark for generative image understanding. *Advances in neural information processing systems*, 36:49659–49678, 2023.
- [48] Meituan LongCat Team, Hanghang Ma, Haoxian Tan, Jiale Huang, Junqiang Wu, Jun-Yan He, Lishuai Gao, Songlin Xiao, Xiaoming Wei, Xiaoqi Ma, et al. Longcat-image technical report. *arXiv preprint arXiv:2512.07584*, 2025.
- [49] Bram Wallace, Meihua Dang, Rafael Rafailov, Linqi Zhou, Aaron Lou, Senthil Purushwalkam, Stefano Ermon, Caiming Xiong, Shafiq Joty, and Nikhil Naik. Diffusion model alignment using direct preference optimization. In *Proceedings of the IEEE/CVF Conference on Computer Vision and Pattern Recognition*, pages 8228–8238, 2024.
- [50] Dianyi Wang, Ruihang Li, Feng Han, Chaofan Ma, Wei Song, Siyuan Wang, Yibin Wang, Yi Xin, Hongjian Liu, Zhixiong Zhang, et al. Deepgen 1.0: A lightweight unified multimodal model for advancing image generation and editing. *arXiv preprint arXiv:2602.12205*, 2026.
- [51] Chenfei Wu, Jiahao Li, Jingren Zhou, Junyang Lin, Kaiyuan Gao, Kun Yan, Sheng-ming Yin, Shuai Bai, Xiao Xu, Yilei Chen, et al. Qwen-image technical report. *arXiv preprint arXiv:2508.02324*, 2025.
- [52] Chenyuan Wu, Pengfei Zheng, Ruiran Yan, Shitao Xiao, Xin Luo, Yueze Wang, Wanli Li, Xiyan Jiang, Yexin Liu, Junjie Zhou, et al. Omnigen2: Exploration to advanced multimodal generation. *arXiv preprint arXiv:2506.18871*, 2025.
- [53] Keming Wu, Sicong Jiang, Max Ku, Ping Nie, Minghao Liu, and Wenhui Chen. Editreward: A human-aligned reward model for instruction-guided image editing. *arXiv preprint arXiv:2509.26346*, 2025.
- [54] Xiaoshi Wu, Yiming Hao, Keqiang Sun, Yixiong Chen, Feng Zhu, Rui Zhao, and Hongsheng Li. Human preference score v2: A solid benchmark for evaluating human preferences of text-to-image synthesis. *arXiv preprint arXiv:2306.09341*, 2023.
- [55] Enze Xie, Junsong Chen, Junyu Chen, Han Cai, Haotian Tang, Yujun Lin, Zhekai Zhang, Muyang Li, Ligeng Zhu, Yao Lu, et al. Sana: Efficient high-resolution image synthesis with linear diffusion transformers. *arXiv preprint arXiv:2410.10629*, 2024.

- [56] Jiazheng Xu, Xiao Liu, Yuchen Wu, Yuxuan Tong, Qinkai Li, Ming Ding, Jie Tang, and Yuxiao Dong. Imagereward: Learning and evaluating human preferences for text-to-image generation. *Advances in Neural Information Processing Systems*, 36:15903–15935, 2023.
- [57] Zeyue Xue, Jie Wu, Yu Gao, Fangyuan Kong, Lingting Zhu, Mengzhao Chen, Zhiheng Liu, Wei Liu, Qiushan Guo, Weilin Huang, et al. Dancegrp: Unleashing grp on visual generation. *arXiv preprint arXiv:2505.07818*, 2025.
- [58] Yang Ye, Xianyi He, Zongjian Li, Bin Lin, Shenghai Yuan, Zhiyuan Yan, Bohan Hou, and Li Yuan. Imgedit: A unified image editing dataset and benchmark. *arXiv preprint arXiv:2505.20275*, 2025.
- [59] Tianwei Yin, Michaël Gharbi, Taesung Park, Richard Zhang, Eli Shechtman, Fredo Durand, and Bill Freeman. Improved distribution matching distillation for fast image synthesis. *Advances in neural information processing systems*, 37:47455–47487, 2024.
- [60] Tianwei Yin, Michaël Gharbi, Richard Zhang, Eli Shechtman, Fredo Durand, William T Freeman, and Taesung Park. One-step diffusion with distribution matching distillation. In *Proceedings of the IEEE/CVF conference on computer vision and pattern recognition*, pages 6613–6623, 2024.
- [61] Zhixiong Yue, Zixuan Ni, Feiyang Ye, Jinshan Zhang, Sheng Shen, and Zhenpeng Mi. Know your step: Faster and better alignment for flow matching models via step-aware advantages. *arXiv preprint arXiv:2602.01591*, 2026.
- [62] Yang Zhao, Yanwu Xu, Zhisheng Xiao, Haolin Jia, and Tingbo Hou. Mobilediffusion: Instant text-to-image generation on mobile devices. In *European Conference on Computer Vision*, pages 225–242. Springer, 2024.